

UCLA

UCLA Previously Published Works

Title

Trimethyllysine Reader Proteins Exhibit Widespread Charge-Agnostic Binding via Different Mechanisms to Cationic and Neutral Ligands.

Permalink

<https://escholarship.org/uc/item/57q026rk>

Journal

Journal of the American Chemical Society, 146(5)

Authors

Travis, Christopher
Kean, Kelsey
Albanese, Katherine
et al.

Publication Date

2024-02-07

DOI

10.1021/jacs.3c10031

Peer reviewed



Published in final edited form as:

J Am Chem Soc. 2024 February 07; 146(5): 3086–3093. doi:10.1021/jacs.3c10031.

Trimethyllysine reader proteins exhibit widespread charge-agnostic binding via different mechanisms to cationic and neutral ligands

Christopher R. Travis^a, Kelsey M. Kean^{a,^}, Katherine I. Albanese^a, Hanne C. Henriksen^a, Joseph W. Treacy^b, Elaine Y. Chao^b, K. N. Houk^b, Marcey L. Waters^{a,*}

^aDepartment of Chemistry, CB 3290, University of North Carolina at Chapel Hill, Chapel Hill, NC 27599, USA

^bDepartment of Chemistry and Biochemistry, University of California at Los Angeles, Los Angeles, CA 90095-1569, USA

Abstract

In the last 40 years, cation– π interactions have become part of the lexicon of noncovalent forces that drive protein binding. Indeed, tetraalkylammoniums are universally bound by aromatic cages in proteins, suggesting that cation– π interactions are a privileged mechanism for binding these ligands. A prominent example is the recognition of histone trimethyllysine (Kme3) by the conserved aromatic cage of reader proteins, dictating gene expression. However, two proteins have recently been suggested as possible exceptions to conventional understanding of tetraalkylammonium recognition. To broadly interrogate the role of cation– π interactions in protein binding interactions, we report the first large-scale comparative evaluation of reader proteins for a neutral Kme3 isostere, experimental and computational mechanistic studies, and structural analysis. We find unexpected widespread binding of readers to a neutral isostere, with the first examples of readers that bind the neutral isostere more tightly than Kme3. We find no single factor dictating charge selectivity, demonstrating the challenge of predicting such interactions. Further, readers that bind both cationic and neutral ligands differ in mechanism: binding Kme3 via cation– π interactions and the neutral isostere through the hydrophobic effect

*Corresponding Author Marcey L. Waters – Department of Chemistry, CB 3290, University of North Carolina at Chapel Hill, Chapel Hill, NC 27599, mlwaters@email.unc.edu.

Christopher R. Travis – Department of Chemistry, CB 3290, University of North Carolina at Chapel Hill, Chapel Hill, NC 27599, USA

Kelsey M. Kean – Department of Chemistry, CB 3290, University of North Carolina at Chapel Hill, Chapel Hill, NC 27599, USA[^]

Katherine I. Albanese – Department of Chemistry, CB 3290, University of North Carolina at Chapel Hill, Chapel Hill, NC 27599, USA

Hanne C. Henriksen – Department of Chemistry, CB 3290, University of North Carolina at Chapel Hill, Chapel Hill, NC 27599, USA

Joseph W. Treacy – Department of Chemistry and Biochemistry, University of California at Los Angeles, Los Angeles, CA 90095-1569, USA

Elaine Y. Chao – Department of Chemistry and Biochemistry, University of California at Los Angeles, Los Angeles, CA 90095-1569, USA

K. N. Houk – Department of Chemistry and Biochemistry, University of California at Los Angeles, Los Angeles, CA 90095-1569, USA

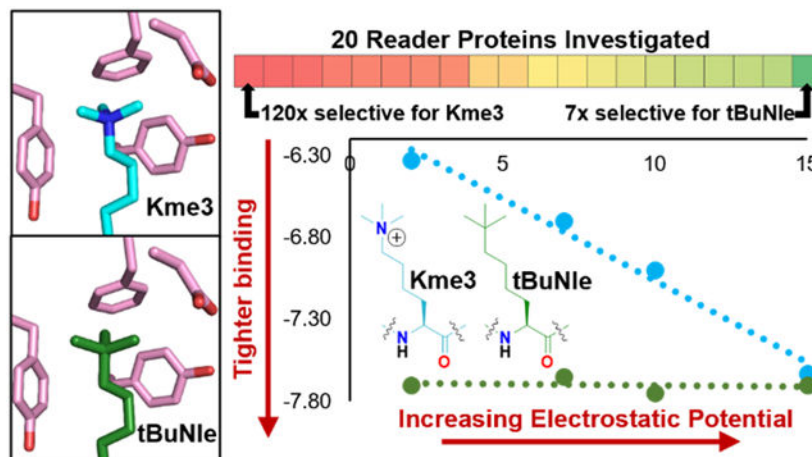
[^]Present Address K.M.K.: Department of Chemistry, High Point University, High Point, NC 27268, USA

Supporting Information. Materials and methods, ESI-LCMS of peptides and proteins, microarray results, ITC curves, protein crystallography data, computational calculations. This material is available free of charge via the Internet at <http://pubs.acs.org>.

The authors declare no competing financial interest.

in the same aromatic cage. This discovery explains apparently contradictory results in previous studies, challenges traditional understanding of molecular recognition of tetraalkylammoniums by aromatic cages in myriad protein-ligand interactions, and establishes a new framework for selective inhibitor design by exploiting differences in charge-dependence.

Graphical Abstract



INTRODUCTION

Methyllysine (Kme) reader proteins bind to this key post-translational modification (PTM) on histone tails in a sequence-selective manner, resulting in recruitment of proteins to the nucleosome that dictate gene expression and elicit downstream effects.¹⁻⁷ Given their significant roles in epigenetic pathways, dysregulation of histone Kme readers is associated with numerous diseases, and many of these proteins have emerged as therapeutic targets.⁸⁻¹⁰ Approximately 200 human histone Kme readers have been characterized to date,^{1,2,11,12} many of which bind the same PTM at the identical histone tail residue, yet elicit distinct biological outcomes.¹³

Several reports describe medicinal chemistry efforts targeting Kme readers.¹⁴⁻¹⁹ However, selectivity remains a major obstacle, as all known Kme3 readers bind the quaternary ammonium group within a conserved aromatic cage (Figure 1a) as well as through cooperative interactions with the surrounding sequence.^{1,2} To date, no therapeutics targeting histone Kme reader proteins have been approved for treatment.²⁰⁻²² Given the well-documented challenges faced in developing selective inhibitors for this class of proteins,²²⁻²⁶ a thorough understanding of the binding capabilities of the aromatic cages of Kme3 readers is warranted to provide insight into novel approaches to achieve selective inhibition.

For nearly 40 years, mechanistic studies of the molecular recognition of quaternary ammonium ions, including Kme3, have repeatedly demonstrated that aromatic cages in proteins as well as synthetic systems preferentially bind cationic ligands over neutral ligands, emphasizing the critical importance of cation- π interactions to these binding

events.²⁷⁻³⁸ As Dougherty described early on, the interaction of quaternary ammonium ions with aromatic rings is multifactorial, consisting of dispersion forces and desolvation costs, as well as an electrostatic component between the cation and the quadrupole moment of the aromatic ring.^{30,39} However, the electrostatic component is the defining feature that distinguishes cation- π interactions from interactions driven by van der Waals interactions or the hydrophobic effect alone. Moreover, studies in a wide range of systems have shown that this additional electrostatic effect overcomes the higher desolvation cost of a quaternary ammonium ion relative to a neutral isostere.^{27,31,32,34-38} In accordance with these studies, maintaining cation- π interactions with a quaternary ammonium ion in the ligand has been a standard approach to inhibitor development for Kme readers,^{22,26,40} as well as other proteins which bind trimethylammoniums in aromatic cages.^{28,29} However, recently a few isolated examples have been reported that draw into question the preference of aromatic cages for cationic ligands.⁴¹⁻⁴³ Moreover, conflicting mechanistic explanations have been proposed, such as binding being driven by displacement of high energy water molecules in the aromatic cage regardless of the nature of the ligand.⁴¹ Because of the biological and medicinal relevance of these interactions as well as the fundamental significance of cation- π interactions in mediating recognition of tetraalkylammoniums in biological systems, we undertook a comprehensive screen of Kme reader protein selectivity for Kme3 vs its neutral isostere tert-butyl norleucine (tBuNle) coupled with mechanistic and structural studies to determine the driving force for aromatic cages binding cationic vs neutral ligands. We find that 10 out of 20 proteins identified from the screen, amounting to approximately 5% of methyllysine reader proteins in humans,¹² bind to the uncharged tBuNle with affinity comparable to or tighter than to Kme3. Indeed, several proteins we report here are the first examples of the neutral isostere binding *more tightly* than Kme3. Furthermore, we find that recognition of cationic and neutral ligands is mechanistically different, with readers binding Kme3 via cation- π interactions and tBuNle via the hydrophobic effect alone. Finally, we find that there is no one structural feature that dictates selectivity. Together, these findings demonstrate a complex molecular recognition profile by aromatic cages that bind trimethylammoniums and explains apparently contradictory results in the literature.^{27,41} Moreover, this work enables novel strategies to selectively target a subset of aromatic-cage containing proteins that are charge-agnostic in binding.

RESULTS AND DISCUSSION

Many methyllysine readers bind histone tails containing a neutral Kme3 analog.

To determine the scope of histone Kme readers that bind the neutral isostere of Kme3, we performed a qualitative screen of biotinylated H3 peptides, each containing Kme3 or tBuNle at the K4 or K9 position, against a reader protein microarray that contains approximately 200 different human proteins that are known or predicted binders of histone methylation (Figure 1c, Figures S1, S2).¹⁶ Results indicate that many histone Kme readers bind to H3K4tBuNle and H3K9tBuNle, suggesting the ability of these readers to bind a neutral ligand is more widespread than previously known.^{41,42}

Twenty histone Kme readers were selected for quantitative analysis of binding to Kme3 and tBuNle histone peptides via isothermal titration calorimetry (ITC) (Figures S3, S4, S5). We

found selectivities ranging from > 120:1 in favor of Kme3 to nearly 7:1 in favor of tBuNle among these proteins (Table 1, Figure S6). The degree of selectivity differs among families: all chromodomains investigated preferentially bind Kme3 whereas readers from the plant homeodomain (PHD) and Tudor domain (TTD) families exhibit a range of selectivities. Eight PHDs bind tBuNle with comparable or tighter affinity than Kme3 (DIDO1, RAG2, BPTF, and ING1/2/3/4/5), while three members of this family demonstrate greater than 2-fold preference for Kme3 (TAF3, JARID1A, and JARID1B). Among the TTDs, SGF29 preferentially binds tBuNle, while JMJD2A and SPIN1 have large preferences for Kme3. Further, we find that the UHRF1 TTD, a key oncological target,⁴⁴ binds H3K9tBuNle nearly 7-fold more tightly than H3K9me3, the largest degree of preference observed for tBuNle of any protein, as well as the only H3K9me3 reader to prefer tBuNle. These results are unexpected, as each of the readers investigated contains a highly conserved cage of two to four aromatic residues in which Kme3 binds, yet these proteins, even those in the same family, differ substantially in their affinities for tBuNle. Mechanistic studies and structural analyses were undertaken to assess factors which dictate this range of selectivities.

Kme3 and tBuNle bind by different mechanisms.

The cation- π interaction has been shown to be the key driving force for binding Kme3 in several readers.^{27,41,45,46} Thus, for proteins which bind tBuNle with equal or tighter affinity, the question arises as to the driving force of binding these two differently charged ligands. For example, it may be that those proteins that bind tBuNle with similar affinity do not bind Kme3 via cation- π interactions due to nonoptimal cation- π geometries, as geometry has been shown to alter strength and electrostatic tunability of this interaction type in previous studies.⁴⁵ We noted that ΔH and ΔS from ITC data indicates that two proteins, the DIDO1 and ING3 PHDs, display enthalpy-entropy compensation (EEC), with similar free energies of binding to Kme3 and tBuNle, but distinct differences in enthalpy and entropy of binding (Figure S6). For these proteins, binding of Kme3 is more enthalpically favorable while binding of tBuNle has a significantly reduced enthalpic driving force and a favorable entropy of binding, consistent with a hydrophobic driving force. Other proteins, including the BPTF PHD, also bind tBuNle with comparable affinities, but do not demonstrate significant EEC (Figure S6). While the observed EEC for some proteins suggests possible differences in mechanism, these data alone are not sufficient to draw a definitive conclusion, as EEC is not a consistently reliable measure of the hydrophobic driving force.⁴⁷ Thus, we pursued a more rigorous method to evaluate the binding mechanisms of readers to Kme3 and tBuNle.

To gain further insight into the mechanisms of binding of the unselective readers, we turned to tuning the electrostatics of aromatic residues, which is an established strategy to evaluate cation- π interactions.⁴⁸⁻⁵² Previously, we developed a genetic code expansion (GCE) methodology incorporating *para*-substituted Phe derivatives⁴⁵ to systematically tune the electrostatic potentials (ESP) of aromatic residues within cages of readers, which provides information on the electrostatic contribution to binding at the individual residue level (Figure 2). This approach has elucidated the driving forces of various reader proteins binding to different PTMs,^{53,54} including cation- π interactions with Kme3.^{45,46} Using this GCE method, we investigated the DIDO1 PHD and the SGF29 TTD (Figure 2). We prepared

a series of DIDO1 PHD Tyr8 mutants and SGF29 TTD Tyr238 mutants via GCE,⁵⁵ and measured binding to H3K4me3 and H3K4tBuNle peptides via ITC (Figure 2, Figure S5).

The DIDO1 PHD domain series of Tyr8 mutants exhibits significant differences in binding affinity to the Kme3 peptide, with electron-withdrawing groups resulting in weaker binding. Plotting the free energy of binding (G_{binding}) against the calculated ESP value⁵⁶ of each Tyr8 mutant results in a linear free energy relationship (LFER), indicating that binding is driven by electrostatically tunable cation- π interactions (Figure 2, Figure S7). The slope of this interaction, which indicates the degree of electrostatic influence on binding, is comparable to previously studied readers binding Kme3.^{45,46} In contrast, plotting G_{binding} for tBuNle with the series of Tyr8 mutants against ESP results in a flat line, indicating that electrostatics have no influence on binding to this ligand (Figure 2). These results demonstrate that the DIDO1 PHD binding Kme3 is dependent on cation- π interactions as has been observed in other Kme3 readers, while this protein binds to tBuNle via the hydrophobic effect alone, which is independent of electrostatics, in agreement with observed EEC (Figure S6). Similarly, for the SGF29 TTD, reduction in the ESP in a series of Tyr238 mutants also correlates to decreased binding affinities to the Kme3 peptide, consistent with tunable cation- π interactions (Figure 2, Figure S7), whereas binding to tBuNle by the SGF29 TTD is not significantly affected by mutations at Tyr238. Together, GCE studies indicate that both proteins, which are from two different families, utilize different mechanisms to recognize Kme3 versus tBuNle within the same aromatic cage binding motif, even though the wild-type G_{binding} to the two ligands is similar. To gain further insight, we performed energy decomposition analysis calculations on SGF29 TTD binding the two ligands at the M06-2X/6-311++G(d,p), SMD(Water) level of theory. These results demonstrate that binding to the two ligands differs primarily in the contribution of electrostatics and desolvation to the interaction, providing further support for different mechanisms of binding (Figure 3a, Figure S8). This finding, that the same aromatic cage binds cationic and neutral ligands with comparable affinities but by different mechanisms, is striking.

Further analysis of the contribution of the cation- π interaction was accomplished through a double mutant cycle (Figure S9) using tBuNle as the Kme3 mutation, as it lacks a cation, and *p*NO₂Phe as the Tyr mutation, as it lacks a significant electrostatic contribution with an ESP value near zero (Figure 2b). This novel approach allows us to quantify cation- π interactions for a single aromatic residue. The contribution of the cation- π interaction to binding is estimated to be -2.3 ± 0.1 kcal/mol for Tyr8 in DIDO1 PHD and -1.3 ± 0.2 kcal/mol for Tyr238 in SGF29 TTD. This emphasizes that although these proteins bind with comparable or tighter affinity to the neutral ligand, cation- π interactions are still significant in binding Kme3. Moreover, these results emphasize that measuring binding of tBuNle to wild-type protein is not a sufficient mechanistic tool for probing the contribution of cation- π interactions.

Neutral isostere binds in the same pocket as Kme3.

We solved a 1.3 Å resolution crystal structure of the RAG2 PHD bound to H3K4tBuNle (Figure 3b, PDB 8T4R) that exhibits a highly similar conformation to this protein binding

Kme3 (PDB 2V89), emphasizing that tBuNle does not access a different binding site or contacts than Kme3 while binding with comparable affinity (Figure 3, Figure S10).⁵⁷ This is in agreement with previously determined structures with tBuNle that overlay with Kme3 (Figure S8).⁴¹

Acidic residues in the binding pocket do not predict charge preference.

We evaluated whether the presence of an acidic residue near a reader's aromatic cage may drive selectivity for Kme3 through a favorable electrostatic interaction between the cationic ligand and the anionic acidic residue and/or unfavorable desolvation of the acidic residue upon binding of tBuNle.⁵⁸ Multiple Kme3 readers have an acidic residue within 5 Å of a methyl or methylene group on the ϵ -N of Kme3 and are selective for Kme3 (Figure S11). However, that is not sufficient to dictate a preference for Kme3. For example, the SGF29 and UHRF1 TTDs each contain an acidic residue in their aromatic cage 3.4 Å away from the nearest Kme3 methyl group but are not selective for Kme3 (Figures S8, S11, S12). Additionally, several proteins that are selective for Kme3 do not have an acidic residue in the cage, including the JARID1A/B PHDs and the CBX5 chromodomain (Figures S8, S11, S12). Thus, identification of an acidic residue in the aromatic cage does not determine selectivity or lack thereof for Kme3 over tBuNle.

Calculated aromatic cage interactions do not predict charge preference.

Since each reader differs in the number and type of aromatic residues in its cage (Figures S8, S11, S12), and the strengths of cation- π interactions are affected by distance and angle,³⁰ we performed computational studies at the M06-2X/6-311++G(d,p), SMD(Water) level of theory. For each protein with an available structure, we calculated interaction energies (E_{Int}) between Kme3 or tBuNle and each amino acid in the binding pocket (Figures S8, S11, S12). Plotting the sum of the E_{Int} for each interaction in the cage versus the experimental $\Delta G(Kme3/tBuNle)$ resulted in minimal correlation (Figures S11, S13), indicating that stronger structurally predicted cation- π interactions (i.e. larger summed E_{Int}) do not correlate with increased selectivity for Kme3.

Interactions with the surrounding histone tail do not predict charge preference.

Given that Kme readers bind histones through cooperative interactions with both Kme3 and the surrounding sequence, we considered whether readers which have lower selectivity for histones containing Kme3 over unmodified lysine may also be less selective for Kme3 over tBuNle. Comparison of the ratio of the K_D of binding to Kme3 versus the unmodified H3 tail (based on literature values, Figure S11) to the ratio of binding to Kme3 and tBuNle shows no correlation, suggesting that differences in binding to the sequence surrounding Kme3 do not dictate reader protein selectivity for Kme3 vs tBuNle (Figure S14). Furthermore, the five ING PHDs, which have nearly identical aromatic cages (Figure S15) but differ in residues that interface with the surrounding histone tail,⁵⁹ demonstrate similar selectivity profiles (Table 1), indicating that differences in interactions with the histone tail outside of the aromatic cage do not dictate preference for Kme3 vs tBuNle.

In sum, no single unifying feature dictates selectivity for Kme3 vs tBuNle. Instead, differences in many contributing interactions, which amount to a sum of small differences

in G_{binding} , contribute to the range of selectivities observed for the 20 proteins that were investigated. This work elucidates that the aromatic cages of Kme3 readers are significantly more complex than previously thought and that simple structural analysis is not sufficient to predict selectivity for Kme3 vs tBuNle. Interestingly, a study of the histone sequence selectivity, rather than PTM recognition, by chromodomains, came to a related conclusion that no single structural feature of the reader protein outside of the aromatic cage explains binding preferences.⁶⁰

CONCLUSION

Through a microarray screen and quantitative biophysical studies, we demonstrate that the binding of histone Kme3 readers to the neutral tBuNle isostere is widespread, with the aromatic cages of ~5% of human Kme readers binding tBuNle with comparable or tighter affinity than Kme3. Additionally, this is the first report of aromatic cages which recognize trimethylammoniums preferentially binding a neutral ligand, contrasting long-standing precedent that this structural motif preferentially binds charged ligands.^{27,31,32,34-38} Moreover, we find that there are significant differences in selectivity for Kme3 vs tBuNle between proteins with highly similar aromatic cages, proteins from the same family, and proteins which recognize the same sequence on the histone tail.

Our studies demonstrate differences in binding mechanisms to these two ligands, utilizing electrostatically tunable cation- π interactions to bind Kme3 versus solely using the hydrophobic effect to recognize tBuNle. Despite the universal nature of aromatic cages in binding Kme3, we find that no individual structural feature is responsible for the wide range of selectivities for Kme3 versus tBuNle observed. This is an example in which Ockham's Razor, which advocates for simpler explanations over those that are more complex, is not supported.⁶¹ This work emphasizes the challenge of extrapolating findings from one molecular recognition system to others as it shows that small differences in the host or protein can result in significant differences in guest or ligand binding. Moreover, these experimental data are important to inform computational and artificial intelligence models of the binding profiles of aromatic cages, a key structural motif across biology.

This work establishes a new framework for the design of selective inhibitors by exploiting differences in charge-dependence among readers in the same family with highly similar binding pockets, which may address a recurrent challenge in therapeutically targeting Kme3 readers. For example, we discovered only a single H3K9me3 reader, the UHRF1 TTD, preferentially recognizes tBuNle, offering a promising starting point for therapeutic development for this significant oncological target.^{17,44} Moreover, these findings may have broader implications beyond histone Kme3 reader proteins, as evolution has converged on aromatic cages to bind small molecules containing trimethylammonium groups, including acetylcholine, choline, betaine, carnitine, and others;^{34,62-64} many of these binding events have been shown to be primarily driven by cation- π interactions.^{27-29,31,32,34,35} Since there is no selective pressure for these proteins to preferentially bind a cationic ligand over a neutral analog, the variable ability of different aromatic cages to bind a neutral analog of a trimethylammonium may extend to other classes of proteins. Our findings provide new

insight into potential approaches for targeting aromatic cages and indicate the need to further analyze other classes of proteins that bind trimethylammonium-containing ligands.

Supplementary Material

Refer to Web version on PubMed Central for supplementary material.

ACKNOWLEDGMENT

This work was funded by National Institute of General Medical Sciences of the National Institutes of Health under award numbers R01 GM118499 and R35 GM145227 to M.L.W. and K12-GM000678 to K.M.K, as well as the National Institute of Allergy and Infectious Diseases under award number R01 AI141481 to K.N.H. C.R.T. was supported by the NSF Graduate Research Fellowship Program (GRFP). K.I.A. was supported in part by a Burroughs Wellcome Fellowship. Microarray experiments were conducted in the Protein Array and Analysis Core (PAAC) at the University of Texas MD Anderson Cancer Center, which is supported by a grant from the Cancer Prevention and Research Institute of Texas (CPRIT RP 180804). The authors thank Dr. Mark Bedford (UT MD Anderson) for assistance with microarray experiments. This work used computational and storage services associated with the Hoffman2 Shared Cluster provided by the UCLA Institute for Digital Research and Education's Research Technology Group. ITC experiments were conducted at the Macromolecular Interactions Facility at the University of North Carolina at Chapel Hill, which is supported by the National Cancer Institute of the National Institutes of Health under award number P30CA016086. Crystallography data were collected at Southeast Regional Collaborative Access Team (SER-CAT) 22-ID beamline at the Advanced Photon Source, Argonne National Laboratory. SER-CAT is supported by its member institutions, and equipment grants (S10_RR25528, S10_RR028976 and S10_OD027000) from the National Institutes of Health. Use of the Advanced Photon Source was supported by the U. S. Department of Energy, Office of Science, Office of Basic Energy Sciences, under Contract No. W-31-109-Eng-38. The authors thank Dr. Ashutosh Tripathy for assistance with ITC experiments.

ABBREVIATIONS

Kme3	trimethyllysine
tBuNle	tert-butyl norleucine
H3	histone 3
ESP	electrostatic potential
ITC	isothermal titration calorimetry
EEC	enthalpy-entropy compensation
GCE	genetic code expansion

REFERENCES

1. Taverna SD, Li H, Ruthenburg AJ, Allis CD & Patel DJ How chromatin-binding modules interpret histone modifications: lessons from professional pocket pickers. *Nature structural & molecular biology* 14, 1025–1040 (2007).
2. Musselman CA, Lalonde M-E, Côté J & Kutateladze TG Perceiving the epigenetic landscape through histone readers. *Nature structural & molecular biology* 19, 1218–1227 (2012).
3. Musselman CA, Khorasanizadeh S & Kutateladze TG Towards understanding methyllysine readout. *Biochimica et Biophysica Acta (BBA)-Gene Regulatory Mechanisms* 1839, 686–693 (2014). [PubMed: 24727128]
4. Luger K, Mäder AW, Richmond RK, Sargent DF & Richmond TJ Crystal structure of the nucleosome core particle at 2.8 Å resolution. *Nature* 389, 251–260 (1997). [PubMed: 9305837]
5. Campos EI & Reinberg D Histones: annotating chromatin. *Annual review of genetics* 43, 559–599 (2009).

6. Rothbart SB & Strahl BD Interpreting the language of histone and DNA modifications. *Biochimica et Biophysica Acta (BBA)-Gene Regulatory Mechanisms* 1839, 627–643 (2014). [PubMed: 24631868]
7. Strahl BD & Allis CD The language of covalent histone modifications. *Nature* 403, 41–45 (2000). [PubMed: 10638745]
8. Chi P, Allis CD & Wang GG Covalent histone modifications—miswritten, misinterpreted and mis-erased in human cancers. *Nature reviews cancer* 10, 457–469 (2010). [PubMed: 20574448]
9. Dawson MA, Kouzarides T & Huntly BJ Targeting epigenetic readers in cancer. *New England Journal of Medicine* 367, 647–657 (2012). [PubMed: 22894577]
10. Audia JE & Campbell RM Histone modifications and cancer. *Cold Spring Harbor perspectives in biology* 8, a019521 (2016). [PubMed: 27037415]
11. Murn J & Shi Y The winding path of protein methylation research: milestones and new frontiers. *Nature Reviews Molecular Cell Biology* 18, 517–527 (2017). [PubMed: 28512349]
12. Barnash KD, James LI & Frye SV Target class drug discovery. *Nature chemical biology* 13, 1053–1056 (2017). [PubMed: 28926557]
13. Ruthenburg AJ, Allis CD & Wysocka J Methylation of lysine 4 on histone H3: intricacy of writing and reading a single epigenetic mark. *Molecular cell* 25, 15–30 (2007). [PubMed: 17218268]
14. Wagner EK, Nath N, Flemming R, Feltenberger JB & Denu JM Identification and characterization of small molecule inhibitors of a plant homeodomain finger. *Biochemistry* 51, 8293–8306 (2012). [PubMed: 22994852]
15. Zhang MY et al. Covalent labeling of a chromatin reader domain using proximity-reactive cyclic peptides. *Chemical Science* 13, 6599–6609 (2022). [PubMed: 35756531]
16. Bae N. et al. Developing Spindlin1 small-molecule inhibitors by using protein microarrays. *Nature chemical biology* 13, 750–756 (2017). [PubMed: 28504676]
17. Senisterra G. et al. Discovery of small-molecule antagonists of the H3K9me3 binding to UHRF1 tandem tudor domain. *SLAS DISCOVERY: Advancing Life Sciences R&D* 23, 930–940 (2018). [PubMed: 29562800]
18. James LI et al. Discovery of a chemical probe for the L3MBTL3 methyllysine reader domain. *Nature chemical biology* 9, 184–191 (2013). [PubMed: 23292653]
19. Stuckey JI et al. A cellular chemical probe targeting the chromodomains of Polycomb repressive complex 1. *Nature chemical biology* 12, 180–187 (2016). [PubMed: 26807715]
20. Engelberg IA, Foley CA, James LI & Frye SV Improved methods for targeting epigenetic reader domains of acetylated and methylated lysine. *Current opinion in chemical biology* 63, 132–144 (2021). [PubMed: 33852996]
21. Bennett RL & Licht JD Targeting epigenetics in cancer. *Annual review of pharmacology and toxicology* 58, 187–207 (2018).
22. Waybright JM & James LI Getting a handle on chemical probes of chromatin readers. *Future Medicinal Chemistry* 13, 749–763 (2021). [PubMed: 31920100]
23. Santiago C, Nguyen K & Schapira M Druggability of methyl-lysine binding sites. *Journal of computer-aided molecular design* 25, 1171–1178 (2011). [PubMed: 22146969]
24. Milosevich N & Hof F Chemical inhibitors of epigenetic methyllysine reader proteins. *Biochemistry* 55, 1570–1583 (2016). [PubMed: 26650180]
25. James LI & Frye SV Chemical probes for methyl lysine reader domains. *Current opinion in chemical biology* 33, 135–141 (2016). [PubMed: 27348158]
26. Ortiz G, Kutateladze TG & Fujimori DG Chemical tools targeting readers of lysine methylation. *Current Opinion in Chemical Biology* 74, 102286 (2023). [PubMed: 36948085]
27. Hughes RM, Wiggins KR, Khorasanizadeh S & Waters ML Recognition of trimethyllysine by a chromodomain is not driven by the hydrophobic effect. *Proceedings of the National Academy of Sciences* 104, 11184–11188 (2007).
28. Schärer K. et al. Quantification of cation– π interactions in protein–ligand complexes: crystal-structure analysis of factor Xa bound to a quaternary ammonium ion ligand. *Angewandte Chemie International Edition* 44, 4400–4404 (2005). [PubMed: 15952226]

29. Salonen LM et al. Cation– π interactions at the active site of factor Xa: dramatic enhancement upon stepwise N-alkylation of ammonium ions. *Angewandte Chemie International Edition* 48, 811–814 (2009). [PubMed: 19101972]
30. Ma JC & Dougherty DA The cation– π interaction. *Chemical reviews* 97, 1303–1324 (1997). [PubMed: 11851453]
31. Zacharias N & Dougherty DA Cation– π interactions in ligand recognition and catalysis. *Trends in pharmacological sciences* 23, 281–287 (2002). [PubMed: 12084634]
32. Dougherty DA Cation– π interactions involving aromatic amino acids. *The Journal of nutrition* 137, 1504S–1508S (2007). [PubMed: 17513416]
33. Shepodd TJ, Petti MA & Dougherty DA Molecular recognition in aqueous media: donor-acceptor and ion-dipole interactions produce tight binding for highly soluble guests. *Journal of the American Chemical Society* 110, 1983–1985 (1988).
34. Beene DL et al. Cation– π interactions in ligand recognition by serotonergic (5-HT_{3A}) and nicotinic acetylcholine receptors: the anomalous binding properties of nicotine. *Biochemistry* 41, 10262–10269 (2002). [PubMed: 12162741]
35. Infield DT et al. Cation– π interactions and their functional roles in membrane proteins. *Journal of molecular biology* 433, 167035 (2021). [PubMed: 33957146]
36. Hasan F, Cohen S & Cohen J Hydrolysis by acetylcholinesterase. *J. Biol. Chem* 255, 3898–3904 (1980). [PubMed: 7372658]
37. Hasan FB, Elkind J, Cohen S & Cohen J Cationic and uncharged substrates and reversible inhibitors in hydrolysis by acetylcholinesterase (EC 3.1. 1.7). The trimethyl subsite. *Journal of Biological Chemistry* 256, 7781–7785 (1981). [PubMed: 7263627]
38. Cohen SG, Lieberman D, Hasan F & Cohen J 1-Bromopinacolone, an active site-directed covalent inhibitor for acetylcholinesterase. *Journal of Biological Chemistry* 257, 14087–14092 (1982). [PubMed: 7142196]
39. Dougherty DA & Stauffer DA Acetylcholine binding by a synthetic receptor: implications for biological recognition. *Science* 250, 1558–1560 (1990). [PubMed: 2274786]
40. Li J, Moumbock AF & Günther S. Exploring cocrystallized aromatic cage binders to target histone methylation reader proteins. *Journal of Chemical Information and Modeling* 60, 5225–5233 (2020). [PubMed: 32786701]
41. Kamps JJ et al. Chemical basis for the recognition of trimethyllysine by epigenetic reader proteins. *Nature Communications* 6, 1–12 (2015).
42. Albanese KI & Waters ML Contributions of methionine to recognition of trimethyllysine in aromatic cage of PHD domains: implications of polarizability, hydrophobicity, and charge on binding. *Chemical Science* 12, 8900–8908 (2021). [PubMed: 34257891]
43. Zhu Y. et al. Water and the Cation– π Interaction. *Journal of the American Chemical Society* 143, 12397–12403 (2021). [PubMed: 34328320]
44. Ashraf W. et al. The epigenetic integrator UHRF1: on the road to become a universal biomarker for cancer. *Oncotarget* 8, 51946 (2017). [PubMed: 28881702]
45. Baril SA et al. Investigation of trimethyllysine binding by the HP1 chromodomain via unnatural amino acid mutagenesis. *Journal of the American Chemical Society* 139, 17253–17256 (2017). [PubMed: 29111699]
46. Kean KM et al. Systematic Variation of Both the Aromatic Cage and Dialkyllysine via GCE-SAR Reveal Mechanistic Insights in CBX5 Reader Protein Binding. *Journal of Medicinal Chemistry* 65, 2646–2655 (2022). [PubMed: 35014255]
47. Cornish-Bowden A. Enthalpy—entropy compensation: a phantom phenomenon. *Journal of Biosciences* 27, 121–126 (2002). [PubMed: 11937682]
48. Zhong W. et al. From ab initio quantum mechanics to molecular neurobiology: a cation– π binding site in the nicotinic receptor. *Proceedings of the National Academy of Sciences* 95, 12088–12093 (1998).
49. Dougherty DA Unnatural amino acids as probes of protein structure and function. *Current opinion in chemical biology* 4, 645–652 (2000). [PubMed: 11102869]

50. Lee Y-J et al. Genetically encoded fluorophenylalanines enable insights into the recognition of lysine trimethylation by an epigenetic reader. *Chemical Communications* 52, 12606–12609 (2016). [PubMed: 27711380]
51. Galles GD et al. Tuning phenylalanine fluorination to assess aromatic contributions to protein function and stability in cells. *Nature communications* 14, 59 (2023).
52. Meyer EA, Castellano RK & Diederich F Interactions with aromatic rings in chemical and biological recognition. *Angewandte Chemie International Edition* 42, 1210–1250 (2003). [PubMed: 12645054]
53. Krone MW et al. More Than π – π – π Stacking: Contribution of Amide– π and CH– π Interactions to Crotonyllysine Binding by the AF9 YEATS Domain. *Journal of the American Chemical Society* 142, 17048–17056 (2020). [PubMed: 32926780]
54. Travis CR, Francis DY, Williams DC Jr & Waters ML Evaluation of acyllysine isostere interactions with the aromatic pocket of the AF9 YEATS domain. *Protein Science* 32, e4533 (2023). [PubMed: 36482045]
55. Young DD et al. An evolved aminoacyl-tRNA synthetase with atypical polysubstrate specificity. *Biochemistry* 50, 1894–1900 (2011). [PubMed: 21280675]
56. Wheeler SE & Houk K Substituent effects in cation/ π interactions and electrostatic potentials above the centers of substituted benzenes are due primarily to through-space effects of the substituents. *Journal of the American Chemical Society* 131, 3126–3127 (2009). [PubMed: 19219986]
57. Matthews AG et al. RAG2 PHD finger couples histone H3 lysine 4 trimethylation with V (D) J recombination. *Nature* 450, 1106–1110 (2007). [PubMed: 18033247]
58. Zhou H-X & Pang X Electrostatic interactions in protein structure, folding, binding, and condensation. *Chemical reviews* 118, 1691–1741 (2018). [PubMed: 29319301]
59. Champagne KS & Kutateladze TG Structural insight into histone recognition by the ING PHD fingers. *Current drug targets* 10, 432–441 (2009). [PubMed: 19442115]
60. Hard R. et al. Deciphering and engineering chromodomain-methyllysine peptide recognition. *Science advances* 4, eaau1447 (2018). [PubMed: 30417094]
61. Hoffmann R, Minkin VI & Carpenter BK Ockham's razor and chemistry. *International Journal for the Philosophy of Chemistry* 3, 3–28 (1997).
62. Chen C, Malek AA, Wargo MJ, Hogan DA & Beattie GA The ATP-binding cassette transporter Cbc (choline/betaine/carnitine) recruits multiple substrate-binding proteins with strong specificity for distinct quaternary ammonium compounds. *Molecular microbiology* 75, 29–45 (2010). [PubMed: 19919675]
63. Horn C. et al. Molecular determinants for substrate specificity of the ligand-binding protein OpuAC from *Bacillus subtilis* for the compatible solutes glycine betaine and proline betaine. *Journal of molecular biology* 357, 592–606 (2006). [PubMed: 16445940]
64. Oswald C. et al. Crystal structures of the choline/acetylcholine substrate-binding protein ChoX from *Sinorhizobium meliloti* in the liganded and unliganded-closed states. *Journal of Biological Chemistry* 283, 32848–32859 (2008). [PubMed: 18779321]

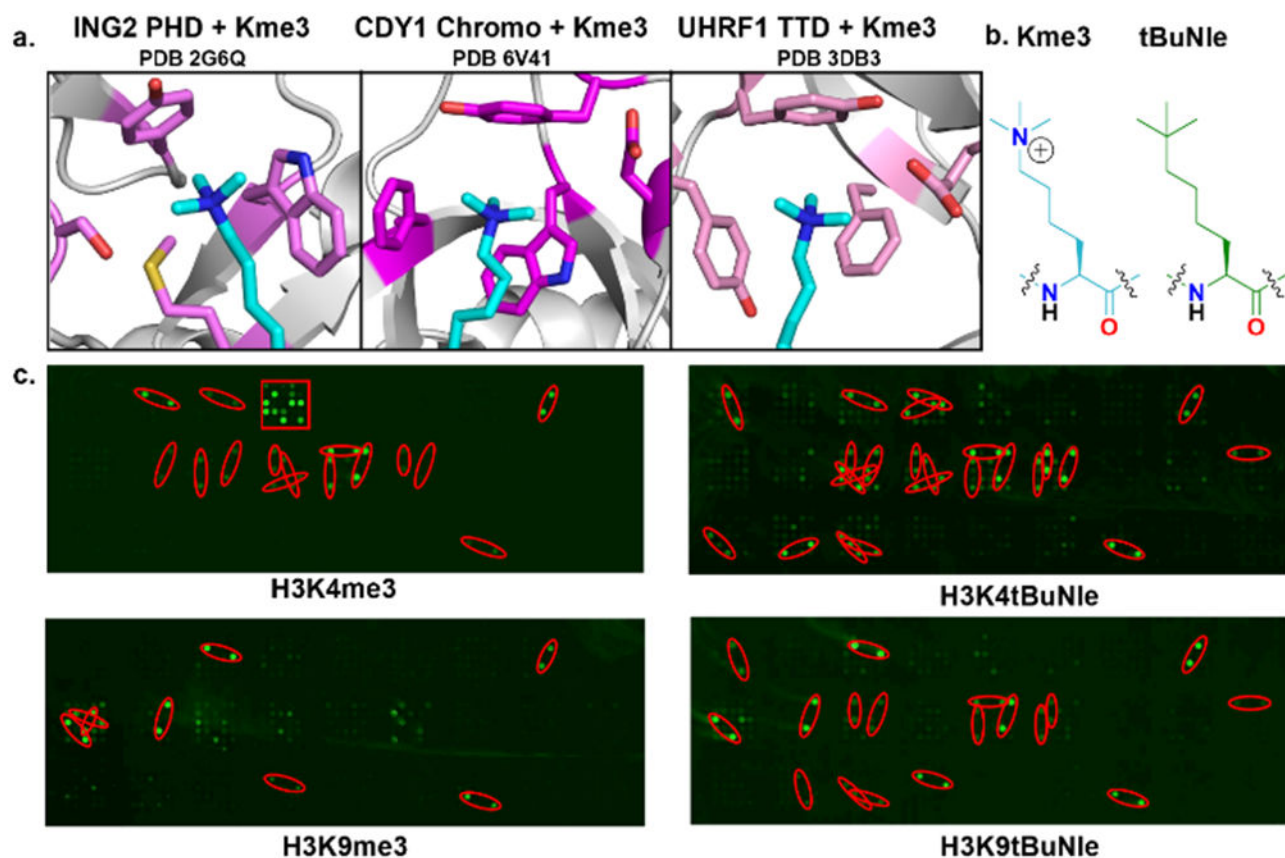
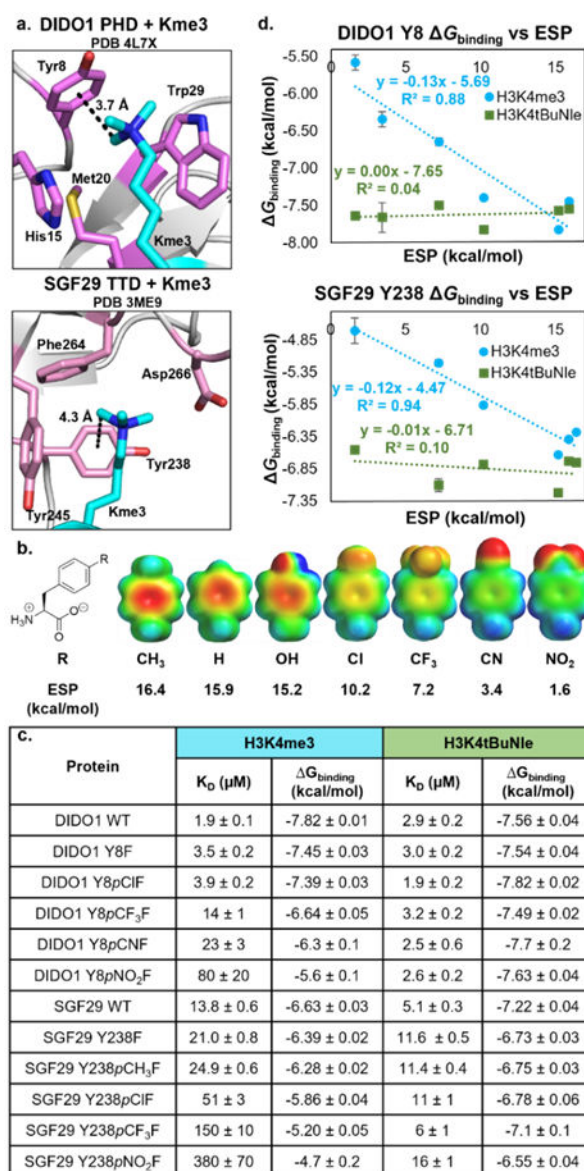


Figure 1.

(a) Aromatic cages of three readers from different families evaluated in this study. (b) Structures of Kme3 and tBuNle. (c) Histone methyllysine reader protein microarray shows many reader proteins from various families are capable of binding the tBuNle mark at H3K4 and H3K9 (significant interactions indicated in red).

**Figure 2.**

(a) Aromatic cages of DIDO1 PHD and SGF29 TTD. (b) Structure of *para*-substituted Phe and ESP maps and values of analogs used in this study. ESP maps were calculated in Spartan using the DFT ωB97X-D/6-31G(d) level of theory with an energetic range from -100 to +100 kcal/mol. Blue indicates positive ESP, green is neutral, and red indicates negative ESP. ESP values were previously reported.⁵⁶ (c) Binding affinities of wild-type and *para*-Phe mutant DIDO1 PHD and SGF29 TTD to H3K4me3 and H3K4tBuNle determined by ITC. Each value reflects the average of three independent ITC experiments, with error as the larger of the standard deviation of the three runs or the largest error from an individual run. (d) LFER plots evaluating the correlation between G_{binding} and calculated ESP values. A portion of (b) was reproduced from reference 46. Copyright 2022 American Chemical Society.

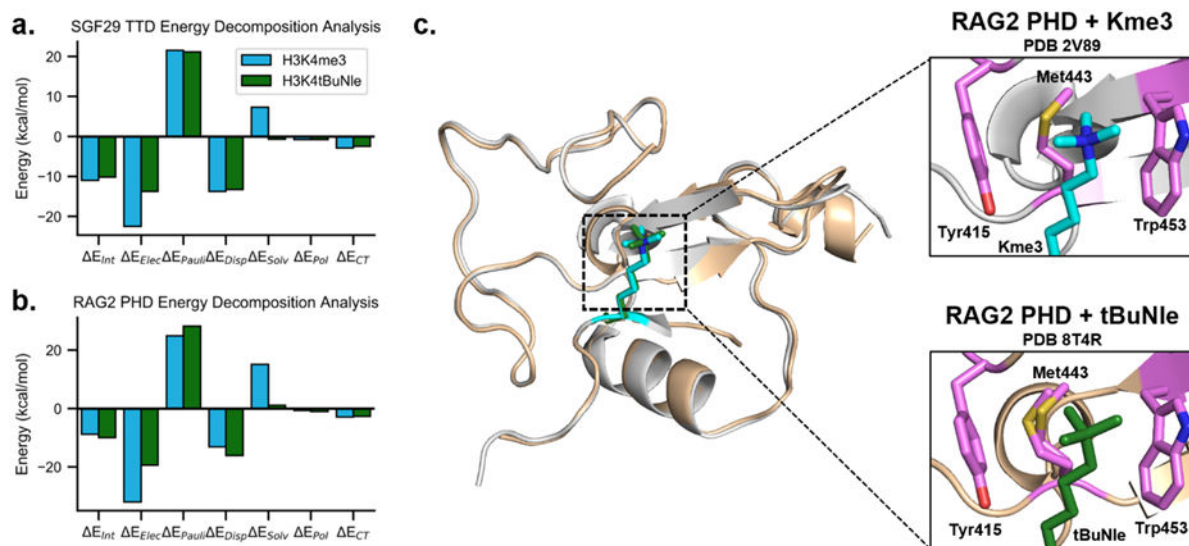


Figure 3. Bar graph of energy decomposition analysis calculations for (a) the SGF29 TTD and (b) RAG2 PHD binding H3K4me3 and H3K4tBuNle calculated at the M06-2X/6-311++G(d,p), SMD(Water) level of theory. (c) Overlay of crystal structures of RAG2 PHD binding to H3K4me3 (cyan, PDB 2V89) and H3K4tBuNle (green, PDB 8T4R).

Table 1.

Binding affinities and selectivities of histone readers binding to H3 peptides containing Kme3 and tBuNle determined by ITC at 25 °C, pH 7.4, 50 mM sodium phosphate, 150 mM (or 500 mM[‡]) NaCl, and 2 mM TCEP. *TAF3 PHD data was previously reported.⁴² ^CBX1 chromodomain data with H3K9me3 was previously reported.⁴⁵

Protein	Ligand	K _D (μM)	K _D (Kme3)/ K _D (tBuNle)	G _{binding} (kcal/mol)
TAF3 PHD*	H3K4me3	1.1 ± 0.2	0.1	-8.16 ± 0.02
	H3K4tBuNle	11 ± 1		-6.78 ± 0.04
JARID1A PHD(3) [‡]	H3K4me3	3.6 ± 0.1	0.46	-7.43 ± 0.01
	H3K4tBuNle	7.9 ± 0.2		-6.96 ± 0.01
JARID1B PHD(3) [‡]	H3K4me3	3.8 ± 0.1	0.46	-7.40 ± 0.01
	H3K4tBuNle	8.2 ± 0.3		-6.94 ± 0.01
DIDO1 PHD	H3K4me3	1.9 ± 0.1	0.66	-7.82 ± 0.01
	H3K4tBuNle	2.9 ± 0.2		-7.56 ± 0.04
RAG2 PHD	H3K4me3	42 ± 6	0.74	-5.98 ± 0.08
	H3K4tBuNle	57 ± 6		-5.79 ± 0.07
BPTF PHD	H3K4me3	8 ± 1	1.2	-7.0 ± 0.1
	H3K4tBuNle	6.6 ± 0.3		-7.07 ± 0.03
ING3 PHD	H3K4me3	2.5 ± 0.1	1.7	-7.64 ± 0.01
	H3K4tBuNle	1.5 ± 0.2		-7.96 ± 0.06
ING2 PHD	H3K4me3	8.5 ± 0.5	2.2	-6.92 ± 0.04
	H3K4tBuNle	3.8 ± 0.1		-7.40 ± 0.02
ING1 PHD	H3K4me3	6.8 ± 0.7	2.8	-7.05 ± 0.06
	H3K4tBuNle	2.4 ± 0.1		-7.67 ± 0.02
ING4 PHD	H3K4me3	10.2 ± 0.6	3	-6.81 ± 0.04
	H3K4tBuNle	3.4 ± 0.2		-7.46 ± 0.03
ING5 PHD	H3K4me3	17.3 ± 0.7	3.3	-6.50 ± 0.01
	H3K4tBuNle	5.2 ± 0.1		-7.21 ± 0.01
CBX1 Chromo [^]	H3K9me3	0.68 ± 0.08	0.017	-8.42 ± 0.03
	H3K9tBuNle	40 ± 10		-6.07 ± 0.09
CHD1 Chromo	H3K4me3	18.8 ± 0.7	0.13	-6.45 ± 0.02
	H3K4tBuNle	150 ± 20		-5.2 ± 0.1
CDY1 Chromo	H3K9me3	1.75 ± 0.08	0.13	-7.85 ± 0.02
	H3K9tBuNle	14 ± 1		-6.63 ± 0.04
CBX5 Chromo	H3K9me3	15 ± 4	0.15	-6.6 ± 0.2
	H3K9tBuNle	~100		>-6
MPP8 Chromo [‡]	H3K9me3	2.5 ± 0.1	0.16	-7.65 ± 0.02
	H3K9tBuNle	15.3 ± 0.6		-6.57 ± 0.03

Protein	Ligand	K_D (μ M)	$K_D(\text{Kme3})/K_D(\text{tBuNle})$	G_{binding} (kcal/mol)
SPIN1 TTD [‡]	H3K4me3	0.67 ± 0.04	0.0079	-8.42 ± 0.01
	H3K4tBuNle	85 ± 10		-5.56 ± 0.07
JMJD2A TTD [‡]	H3K4me3	19.5 ± 0.4	0.039	-6.42 ± 0.01
	H3K4tBuNle	>500		>-5
SGF29 TTD	H3K4me3	13.8 ± 0.6	2.7	-6.63 ± 0.03
	H3K4tBuNle	5.1 ± 0.3		-7.22 ± 0.04
UHRF1 TTD [‡]	H3K9me3	44 ± 3	6.8	-5.94 ± 0.03
	H3K9tBuNle	6.5 ± 0.8		-7.1 ± 0.1